Published in final edited form as:

Circ Res. 2009 March 27; 104(6): 796–804. doi:10.1161/CIRCRESAHA.108.187005.

Mechanistic Insights into Nitrite-Induced Cardioprotection Using an Integrated Metabonomic-Proteomic Approach

David H. Perlman[1,*], **Selena M. Bauer**[2,*], **Houman Ashrafian**[3], **Nathan S. Bryan**[2], **Maria F. Garcia-Saura**[2], **Chee C. Lim**[2,Ψ], **Bernadette O. Fernandez**[2,†], **Giuseppe Infusini**[1], **Mark E. McComb**[1], **Catherine E. Costello**[1], **Martin Feelisch**[2,†]

[1]Cardiovascular Proteomics Center, Center for Biomedical Mass Spectrometry, Boston University School of Medicine, Boston, MA 02118

[2]Whitaker Cardiovascular Institute, Boston University School of Medicine, Boston, MA 02118

[3]Department of Cardiovascular Medicine, Oxford University, Oxford OX3 9DU, UK

Abstract

Nitrite has recently come to the fore as an important bioactive molecule, capable of conferring cardioprotection, as well as a variety of other benefits in the cardiovascular system and elsewhere. The mechanisms by which it accomplishes these functions remain largely unclear. To characterize the dose-response and corresponding cardiac sequelae of transient systemic elevations of nitrite, we assessed the time-course of oxidation/nitros(yl)ation as well as the metabonomic/proteomic and associated functional changes in rat hearts following acute exposure to nitrite *in vivo*. Systemic nitrite elevations resulted in: a) the transient formation of nitroso and nitrosyl species, b) moderate short-term changes in cardiac redox status and c) a pronounced increase in selective oxidative stress as manifested by cardiac ascorbate oxidation persisting long after changes in nitrite-related metabolites had normalized. Glutathione redox status (GSSG/GSH) and the profile of cardioprotection displayed a complex but remarkably concordant dose-response relationship with nitrite. Mass spectrometry-based proteomic studies revealed that nitrite induced significant modifications (including phosphorylation) of specific proteins involved in: i) metabolism (*e.g.*, ALDH2, COQ9, LDH), ii) redox regulation (*e.g.*, PDIA3), iii) contractile function (*e.g.*, Filamin-C), and iv) serine/threonine kinase signaling (*e.g.*, PKA R1α, PP2A A R1-α). Thus, brief elevations in plasma nitrite trigger a concerted cardioprotective response that is characterized by persistent changes in cardiac metabolism, redox stress, and activation of myocardial signaling. These findings help elucidate the possible mechanisms of nitrite-induced cardioprotection and have implications for nitrite dosing in therapeutic regimens.

Address correspondence to: Martin Feelisch, Ph.D., Professor of Experimental Medicine & Integrative Biology, Clinical Sciences Research Institute, Warwick Medical School, The University of Warwick, Gibbet Hill Road, Coventry, CV4 7AL, United Kingdom, Tel: +44 (0)24 7652 8372, Fax: +44 (0)24 7615 0589, mf@warwick.ac.uk.

ΨPresent Address: Vanderbilt University Medical Center, Nashville, TN 37232

†Present Address: Warwick Medical School, University of Warwick, Coventry, CV4 7AL, UK

*These authors contributed equally to this work

Introduction

Although traditionally considered an inert byproduct of nitric oxide (NO) metabolism, the nitrite anion (NO_2^-) is now recognized as an important bioactive molecule.[1] It represents a source of NO, nitrosation and nitrosylation (nitros(yl)ation), yielding profound biological effects, especially in the context of hypoxia and ischemia.[2,3] Nitrite has been shown to elicit NO-dependent vasodilatation,[4,5] angiogenesis[6] and cardioprotection.[7–11] While the mechanisms of cardioprotection afforded by nitrite remain elusive, it has been postulated that nitrite alters the rate of mitochondrial respiration via modulation of the electron transport chain.[7] Nitrite bioconversion to NO has varyingly and non-exclusively been attributed to heme-dependent reductase activity,[7,12,13] to reductase activity contributed by a combination of other enzymes, including aldehyde dehydrogenase (ALDH2) and xanthine oxidase (XO),[14] and to a lesser extent to chemistry occurring at low oxygen tension or low pH.[15] Cardioprotection by nitrite is manifest in isolated heart preparations,[16] and low doses of nitrite prevent ischemia/reperfusion (I/R) injury in myocardial infarction (MI).[17] Thus, while there is great potential for nitrite-based therapeutics, a number of questions remain to be answered: 1) What is the dose-response relationship for nitrite-mediated cardioprotection? 2) What are the immediate (1st hour) and longer-term (24 h) cardiac sequelae of elevations in plasma nitrite levels? 3) By what mechanisms does nitrite-induced cardioprotection occur? Using a metabonomic/proteomic approach, we here demonstrate that, following a brief systemic exposure to nitrite *in vivo*, cardiac tissue experiences a rapid, dose-dependent wave of *S*-, *N*- and heme nitros(yl)ation that is associated with longer-term alterations in redox status and changes in the cardiac proteome that may contribute to cardioprotection.

Methods

An expanded Methods section is available in the online data supplement at http://circres.ahajournals.org.

Animal Care and Nitrite Administration:

Male Wistar rats (Harlan, Indianapolis, IN) were given a single intraperitoneal (i.p.) injection of sodium nitrite dissolved in phosphate buffered saline (PBS, pH 7.4) at doses of 0, 0.1, 1.0 and 10 mg/kg body weight. To avoid effects of chronobiological variation, nitrite injections were staggered for time course experiments such that organ harvest was conducted at the same absolute time-of-day. All animal experiments were performed in triplicate and in accordance with National Institutes of Health Guidelines for the Care and Use of Laboratory Animals and with the Institutional Animal Care and Use Committee of Boston University.

Organ Perfusion and Homogenization:

At 0, 2, 5, 10 and 30 min or 1, 3, 12, 24, 36, and 48 h post-application of nitrite, animals were anesthetized, and organs were perfused before homogenization on ice in the appropriate buffers for metabonomic and proteomic analyses.

Isolated Perfused Heart Preparation:

Hearts were isolated and perfused *ex vivo* in the Langendorff mode using a modified Krebs-Henseleit buffer, according to a previously described protocol.[18] Hearts were stabilized for 15 min and subsequently subjected to 15 min of zero-flow ischemia, followed by 30 min of reperfusion. A custom balloon pressure transducer inserted into the left ventricle was used for measurements of end diastolic pressure (EDP) and rate pressure product (RPP).

Metabonomic and Redox Measurements:

Quantitative analyses of nitroso and nitrosyl species and oxidation products of NO were performed as detailed elsewhere.[19,20] Briefly, nitroso- and nitrosyl- compounds were measured by group-specific denitrosation followed by gas phase chemiluminescence detection. Ascorbate and dehydroascorbate and reduced and oxidized glutathione were measured essentially as described[19]. Protein carbonyls were quantified using a commercially available ELISA (Northwest LLC, Vancouver, WA). Data are means ± SEM from n individual experiments. Statistical analysis was performed by one-way ANOVA using means comparison by Bonferroni. Statistical significance was determined by $P < 0.05$.

Heart Mitochondrial Isolation:

Hearts were perfused, isolated, and homogenized as described[19,20], except using mitochondrial purification buffer (MPB) for homogenization. Crude mitochondria and post-mitochondrial cytoplasm were separated by differential centrifugation.

2D-PAGE Analysis:

2D-PAGE analysis was conducted using IPG strips of pI 3–10 or 4– 7 and 10% SDS-PAGE gels under standard conditions. Gels were stained by Coomassie (Gelcode™ Blue, Pierce, Rockford, IL), silver (PlusOne™ Silver Stain, GE Healthcare), or ProQ-Diamond™ (Invitrogen, Carlsbad, CA). Samples were analyzed on a minimum of three separate gels. Gel images were normalized for total stain intensity within the area of the gels containing distinctly resolved spots and analyzed using QuantityOne™ or PDQuest™ (BioRad).

Western Blotting:

Proteins were transferred to Immobilon-P PVDF membranes (Millipore, Billerica, MA) and probed overnight with a mouse monoclonal anti-nitrotyrosine primary antibody (Upstate, Billerica, MA) at a 1:2500 dilution, followed by horseradish peroxidase-linked anti-mouse secondary antibodies (Upstate) at a 1:4000 dilution.

In-Gel Digestion and MALDI-TOF Mass Spectrometry:

In-gel digestion was conducted as previously described.[21] Briefly, protein spots were subjected to trypsin digestion, followed by peptide extraction and purification using ZipTips™ (Millipore). Mass spectra were obtained using 2,5-dihydroxybenzoic acid as the matrix and AnchorChip™ targets (Bruker-Daltonics, Billerica, MA), using a Reflex IV™ matrix-assisted laser desorption/ionization time-of-flight (MALDI-TOF) MS instrument (Bruker-Daltonics) equipped with a nitrogen laser (337 nm, 3 ns pulse width) in positive ion, reflectron mode, over the range m/z 400–8000.

MS Data Analysis and Peptide Mass Fingerprinting:

MALDI-TOF mass spectra were analyzed using MoverZ™ software (Genomic Solutions; Ann Arbor, MI). Peak lists were submitted to the database search engine Mascot™ (Matrix Science, London, UK) for peptide mass fingerprinting analysis against the SwissProt or NCBI non-redundant protein databases. Only high scoring Mascot™ matches (corresponding to a false positive rate <5%) were considered valid protein assignments.

Preparation of Peptides from Tissue Homogenates and Phosphopeptide Enrichment for LC-MS

Protein was isolated from pooled vehicle-treated (control) and pooled nitrite-treated heart homogenates by acetone/TCA precipitation, then subjected to thiol reduction and alkylation, followed by sequential in-solution digestion with Lys-C (Pierce) and trypsin. Phosphopeptides were enriched using a 2-stage process consisting of calcium phosphate precipitation[22] followed by titanium dioxide enrichment.[23]

Nanoflow HPLC-coupled Tandem Mass Spectrometry

LC-MS was performed on the phosphopeptide-enriched samples using a nanoAcquity UPLC™ capillary high-performance liquid chromatography system (Waters Corp., Milford, MA) coupled to an LTQ-Orbitrap™ hybrid mass spectrometer (ThermoFisher Scientific, San Jose, CA) equipped with a TriVersa NanoMate ion source (Advion, Ithaca, NY). Mass spectra were acquired in the positive-ion mode over the range m/z 300–2000 at a resolution of 60,000. Mass accuracy after internal calibration was within 4 ppm. Tandem mass spectra (MS/MS) were acquired using the LTQ for the five most abundant ions using multistage activation. All spectra were recorded in profile mode for further processing and analysis.

LC-MS and MS/MS Data Analysis

Analysis of LC-MS and MS/MS data was accomplished using Xcalibur and Proteome Discoverer software (ThermoFisher Scientific), while peptide and protein assignments were conducted using Mascot™ against the rodent species subset of the SwissProt database (UniProt release 14.3) employing a error of +/− 6 ppm on precursor ions and +/− 0.6 Da on fragments. Fixed modifications included cysteine carbamidomethylation; variable modifications included phosphorylation and methionine oxidation. Mascot™ results were analyzed using Scaffold (Proteome Software, Portland, OR). Potential phosphopeptides were verified and assignments were refined by manual interpretation of the original spectra.

Results

Acute Systemic Exposure to Nitrite Leads to Rapid, Transient Elevations in Cardiac Tissue Nitrite and Nitros(yl)ation Levels and a Selective, Long-term Perturbation of Cardiac Redox Tone.

We have demonstrated previously that systemically administered nitrite rapidly and dose-dependently equilibrates across multiple organ systems, including the heart, brain, liver, kidney, and lung.[19] Elevated tissue nitrite levels can then directly nitros(yl)ate proteins in an NO-independent manner, an activity that requires the cooperative action of tissue hemes and

thiols.[19] Using an experimental design to model acute systemic nitrite exposure and its cardiac effects (Figure S-1, Online Data Supplement), we extended previous findings by characterizing the dynamics of changes in redox, metabonomic, proteomic, and functional parameters of the heart in response to various doses of nitrite, or vehicle (PBS), over an extended period post administration.

To follow the fate and potential nitrosative and oxidative effects of nitrite after a systemic burst in circulating nitrite concentration, hearts from animals administered a bolus of nitrite (1 mg/kg) were analyzed over a time-course of 48 h post application. At each time point (0, 2, 5, 10, and 30 min, 1, 3, 12, 24, 36, and 48 h), cardiac nitrite levels were measured, together with other NO-related metabolites, including *S*-nitrosothiols and *N*-nitrosoamines (*S*- and *N*-nitroso products) and heme-nitrosyl species. Additionally, as a measure of the cardiac redox tone, the ascorbate oxidation status (the ratio of ascorbic acid over dehydroascorbate) was determined. Analysis of nitrite recovered from perfused heart tissue over the time course showed that there was a rapid increase in cardiac tissue nitrite levels within the first 5 min post administration (Fig. 1). Cardiac nitrite levels peaked between 10 and 30 min (increasing from baseline levels in the high nanomolar range to peak levels in the low micromolar range), remained elevated for a maximum of 1 h, then sharply dropped to baseline levels or below, followed by oscillations near baseline for the remainder of the 48-h period. The short-lived elevations in cardiac nitrite at the early time-points following systemic nitrite administration were accompanied by rapid rises in *S*- and *N*-nitroso and heme-nitrosyl levels (1–3 orders of magnitude from basal values), with *S*-nitroso species undergoing the largest relative changes (Fig. 1). Similar results were observed in other tissues and organs, including brain, liver, kidney, lung, plasma, and erythrocytes (data not shown).

In the heart, these transient nitrite and nitros(yl)ation spikes were associated with a small increase in the ascorbate oxidation status (Fig. 1, asterisk), which returned to near baseline levels within 1 h, consistent with a known direct chemical interaction between ascorbate and nitrite.[24] However, while cardiac nitrite and nitros(yl)ation levels in the subsequent hours remained close to baseline, ascorbate oxidation continued to rise during that time. This progressive increase in ascorbate oxidation peaked at 36 h and remained substantially elevated even 48 h after nitrite administration. Total ascorbate levels changed little over the same period, remaining slightly elevated (15–21%) between the 12-h and 48-h time points. Because this protracted elevation in ascorbate oxidation occurred long after nitrite's return to baseline, it is unlikely to have been caused through direct oxidation by nitrite. Instead, it appears to reflect a lasting change in myocardial redox status potentially mediated by a complex cascade of events elicited by brief systemic exposure to nitrite.

Dose-Response Relationship of Nitrite-Induced Perturbations of Cardiac Redox Tone Is Complex.

Considering the finding that transient, physiologically-relevant elevations in plasma nitrite concentrations are capable of eliciting major, persistent changes in the oxidation status of ascorbate, we sought to characterize these redox perturbations in further detail by examining their dose-response relationship. Nitrite doses (0.1, 1.0, and 10 mg/kg body weight) were

chosen to produce physiologically/pharmacologically relevant rises in plasma concentrations (from nanomolar levels at baseline to treatment levels transiently in the low micromolar range), and concomitant elevations in tissue nitrite levels, as shown previously.[25] Cardiac ascorbate and glutathione oxidation status was analyzed 24 h post-administration of nitrite or vehicle (a time-point at which cardiac nitrite and nitros(yl)ation levels had long returned to near baseline but cardiac ascorbate oxidation was markedly enhanced; see arrow in Fig. 1). Ascorbate oxidation was found to be elevated to comparable levels, independent of the nitrite dose applied (Fig. 2A, left panel). The oxidation status of glutathione was also perturbed following nitrite administration (Fig. 2A, right panel), however, in contrast to that of ascorbate, glutathione showed a complex (trimodal) dose-response relationship. The changes observed were characterized by a decrease in glutathione redox status in hearts exposed to the lowest (0.1 mg/lg) and highest (10 mg/kg) nitrite doses, with essentially no change in hearts exposed to the intermediate (1.0 mg/kg) dose; as with ascorbate, total tissue glutathione concentrations increased slightly (14±4%). No redox changes were observed in time-matched vehicle-treated controls (not shown). To assess potential consequences of the marked changes in ascorbate redox status on global oxidative stress in cardiac tissue, the tissue content of total protein carbonyls was measured 24 h after nitrite application. No significant changes were detected for any of the nitrite doses (data not shown), suggesting that the observed perturbations in oxidant status of the heart were specific to distinct cellular redox couples and did not reflect a global increase in oxidative stress, which would have resulted in increased protein carbonylation.

Only Low and High, But Not Intermediate, Doses of Nitrite Are Cardioprotective.

To evaluate whether the nitrite-induced nitros(yl)ative tissue modifications and perturbations in cardiac redox tone had any effect on the functional properties of the heart, we subjected isolated hearts from nitrite-treated animals to a period of ischemia and assessed their ability to recover during reperfusion. Hearts were obtained 24 h after administration of a bolus dose of nitrite, retrogradely perfused *in vitro,* and, following a 15-min stabilization period, subjected to 15 min of global ischemia. Hearts from animals given a low (0.1 mg/kg) or a high (10 mg/kg) dose of nitrite 24 h prior showed a significant improvement in cardiac contractile recovery during the 30-min reperfusion following zero-flow ischemia. This was reflected in a decreased end diastolic pressure (EDP) (Fig. 2B, left panel) and an increased rate pressure product (RPP) (Fig. 2B, right panel) relative to controls. In contrast, hearts from animals given an intermediate dose (1.0 mg/kg) of nitrite did not differ from hearts of sham-treated animals. Thus, as with the cardiac glutathione oxidation status, functional performance of the heart was affected by prior nitrite exposure in a complex dose-dependent fashion.

Nitrite Induces Alterations to Cardiac Mitochondria-Associated Proteins, PDIA3, COQ9, and ALDH2.

To evaluate what underlies the nitrite-induced changes in myocardial function following I/R, we characterized alterations in the cardiac proteome using a global differential 2D-PAGE-based proteomic analysis. Hearts were analyzed 24 h after exposure to increasing amounts of nitrite. For these experiments, we employed a strategy of partitioning heart tissue into mitochondria (containing metabolic and redox-active proteins) and cytoplasm (containing

soluble contractile/structural proteins) through differential centrifugation. Mitochondria were denatured in IEF buffer and subjected to 2D-PAGE analysis followed by silver staining for high-sensitivity, qualitative differential comparison (Fig. 3). Although largely uniform between treatment groups (as evident by the overall similarity of the stained gels; see Fig. 3A), the cardiac mitochondrial proteome displayed several distinct protein changes in response to nitrite treatment. Among other changes, profound qualitative nitrite dose-dependent changes were consistently evident in three series of protein spots in trains within the pI 4.5–6.5 region of the gels (Fig. S-2 and movies showing dose-dependent changes in spot patterns for each series, Online Data Supplement), suggestive of changes within each series in pI-altering posttranslational modifications (PTMs). Series 1 was located roughly at pI 6 and MW 60 kD and contained four spots (Fig. 3Bi, left panel, spots a-d), Series 2 was located in the region of pI 5 and MW 35 kD and also contained 4 spots (Fig. 3Bii, left panel, spots a-d), while Series 3 was located in the range of pI 6.3 and MW 55 kD and consisted of five spots (Fig. 3Biii, left panel, spots a-e). Interestingly, although in each case pronounced changes in spot intensities within Series 1–3 did occur between dosage groups, the patterns of changes were distinct for each series. For example, while the intensities of the two most acidic spots in Series 1 (Fig. 3Bi, left panel, spots a and b) followed roughly the same dose-dependent behavior as the glutathione oxidation status, the intensities of the two most basic spots in that same series (Fig. 3Bi, left panel, spots c and d) followed the dose-dependence of the ascorbate oxidation status. This suggests that there may be complex mechanisms linking the migrational isoform changes (potentially resulting from changes in PTM) to the ascorbate and glutathione redox status, as well as to functional changes.

To identify the proteins of these spot series, preparative amounts of purified mitochondrial material were subjected to 2D–PAGE analysis followed by Coomassie blue staining. A large-scale peptide mass fingerprint (PMF) survey of the protein spots across the gels was undertaken as a roadmap for protein identifications by excising spots and subjecting them to in-gel digestion, followed by MALDI-TOF MS analysis of eluted peptides and PMF analyses of the MS peak lists using the database search engine, Mascot™, and rodent proteomic databases (see Table 1, Online Data Supplement). When selected spots from each of Series 1–3 were also subjected to these digestion and MALDI-TOF MS analyses (Fig. 3Bi-iii, right panels, from representative spots within each series), PMF results showed that the constituents of the trains of spots in Series 1, 2, and 3 matched unambiguously to isoforms of protein disulfide isomerase A3 (PDIA3), ubiquinone biosynthesis protein CoQ9 (COQ9), and aldehyde dehydrogenase 2 (ALDH2), respectively (having Mascot™ scores of 221, 79, and 205, and corresponding false discovery rates (Expect values) of 1.6×10^{-18}, 8.6×10^{-5}, and 6.2×10^{-17}).

Nitrite Induces Changes in the Nitration and Phosphorylation Status of Cardiac Myofilament, Energetic, and Signaling Proteins.

In addition to mitochondrial analyses, we performed differential 2D-PAGE analyses on post-mitochondrial cytoplasmic supernatants from hearts of nitrite-treated animals. This cytoplasmic cell fraction contains the majority of soluble structural and contractile (including myofilament) proteins of the heart. These 2D gels (Fig. S-3, Online Data Supplement) revealed distinct alterations in spot intensity in a cluster of spots corresponding

to isoforms of myosin light chain protein 1 (MLC1) (Fig. 4A, spots a-g), which varied according to nitrite treatment dose. Importantly, our findings are consistent with previous reports suggesting that similar changes in MLC1 phosphorylation occur in the context of cardioprotection (*e.g.* by adenonsine and diazoxide).[26,27] Qualitative protein migrational changes were also observed in the train of spots corresponding to cardiac α-actin, particularly in acidic isoforms (corresponding potentially to actin phosphospecies or other acidic post-translationally modified isoforms), as highlighted by staining the 2D gels with the dye, Pro-Q Diamond™, which stains protein phospho-isoforms and other acidic species (Fig. 4B, spots a-e). As with the proteomic changes observed in mitochondria, the staining intensity of these actin species varied with nitrite dose. These observations motivated us to undertake a detailed characterization of nitrite-induced PTMs that are typically more stable than nitros(yl)ation.

In the context of oxidative stress, nitrite's capacity to induce protein nitrosation may be accompanied by the formation of nitrogen dioxide and the posttranslational nitration of proteins. To assess whether brief nitrite exposure also leads to a change in nitration of cardiac proteins, we conducted 2D-PAGE followed by anti-nitrotyrosine Western analysis of whole heart homogenates 24 h after treatment with nitrite (Fig. 4C). In order to control for blotting variability, first dimension isoelectric focusing strips from each nitrite-dose sample were placed atop a single second dimension gel and subjected as one to second dimension SDS-PAGE and Western blotting. Nitration was not indiscriminant: the staining intensity of protein spots such as those corresponding to the beta subunit of F1-ATPase and the chaperone protein GRP78 (both known targets of tyrosine nitration) (spots f and g, Fig. 4C) remained unchanged with increasing nitrite exposure, while qualitative changes in anti-nitrotyrosine immunoreactivity were observed for lactate dehydrogenase B (LDH) (spot a, Fig. 4C), dehydrolipamide *S*-acetyl transferase (PDC-E2, a component of the pyruvate dehydrogenase complex) (spot b, Fig. 4C), α-actin (spot c, Fig. 4C), as well as other cardiac proteins (including spots d and e, Fig. 4C). While LDH anti-nitrotyrosine immunoreactivity increased with increasing nitrite dose, the apparent nitration of other proteins showed a more complex, bimodal dose-response relationship (decreasing at low doses, rising at higher doses). Conversely, anti-nitrotyrosine staining of several cardiac proteins was already observed under basal conditions (in vehicle controls). A summary of the changes observed across nitrite doses in the normalized relative intensity of each spot shown in Figures 3B and 4A–C is contained in Table 2, Online Data Supplement.

As the spot patterns we observed in several of our 2D gel analyses (*e.g.*, Fig 3B, Series 1–3) resemble those that are seen in the context of phosphorylation, we investigated whether there was evidence for cardiac phosphoproteomic alterations in response to nitrite administration. Indeed, the MALDI-TOF mass spectra of peptides from the 2D gel spots corresponding to acidic isoforms of PDIA3, COQ9, and ALDH2 (as in Fig 3B, spots a and b) contained ions that would correspond to phosphopeptides derived from these proteins. For example, we detected an ion corresponding to the ALDH2 phosphopeptide, 431–438 (Fig 5A), bearing phosphorylation on residue Thr431, a recently reported phosphosite.[34] Also evident in the MALDI-TOF mass spectra were several other potential phosphopeptides (data not shown) that correspond to phosphorylation at known and novel sites, whose definitive assignments await confirmation and further characterization by other MS techniques.

Recently it has become appreciated that gel-based proteomics can lead to chemical artifacts that resemble protein phosphorylation.[28] In order to avoid potential artifactual chemical modifications associated with peptides extracted from stained gels, tryptic peptides were produced directly from pooled heart homogenates of vehicle-treated (control) animals and pooled homogenates from nitrite-treated animals, by in-solution endoproteinase digestion. Peptides were then subjected to a two-stage phosphopeptide enrichment procedure, involving calcium phosphate precipitation and titanium dioxide purification. Phosphopeptide-enriched samples were then subjected to characterization by liquid chromatography (LC)-MS and tandem MS (MS/MS). LC-MS analysis of the samples from nitrite-treated animals detected the phosphorylated and non-phosphorylated forms of the ALDH2 peptide 431–438 (Fig 5B) that were also found in the gel-derived samples analyzed by MALDI-TOF MS. MS/MS spectra of this and other potential phosphopeptides from ALDH2, PDIA3 or COQ9 were not acquired during the data-driven selection of peaks for MS/MS acquisition due to their low relative abundances in the mass spectra obtained during the LC/MS analyses of the phosphopeptide-enriched heart homogenate material. However, LC-MS/MS analysis did reveal phosphopeptides which were abundantly present in the pooled nitrite-treated samples (Fig. 6), but below detection in the control samples. Interpretation of the MS/MS spectra led to the identification of these phosphopeptides as belonging to Filamin-C (FLNC) (Fig. 6A) and to specific subunits of cAMP-dependent protein kinase (PKA) (Fig 6B) and serine/threonine protein phosphatase 2A (PP2A) (Fig 6C). Because numerous diagnostic fragment ions were present in each spectrum, it was possible to assign unambiguously the sites of phosphorylation to residues Ser2234 of FLNC, Ser83 of PKA Regulatory Subunit 1-alpha (PKA R1α, KAP0), and Ser9 of PP2A Regulatory Subunit A-alpha (PP2A A R1-α, 2AAA) These three proteins were not identified in our 2D-PAGE and PMF analyses, possibly due to the large size of filamin-C, which probably makes it incompatible with our 2D-PAGE methodologies, and the potential co-migration of PKA R1α and PP2A A R1-α with other, much higher abundance proteins (Their MWs and theoretical pIs would place them in the regions of highest spot density in our 2D-PAGE gels. Although numerous additional phosphosites on other proteins were characterized by these LC-MS/MS analyses (such as Ser283 of tropomyosin alpha chain 1, TPM1, and Ser663 of sarcoplasmic/endoplasmic reticulum calcium ATPase 2 (SERCA2), SERCA2A, AT2A2, data not shown), their abundances did not appear to vary substantially with nitrite treatment.. Further studies, such as MS analyses incorporating stable-isotope labelled standards, will be necessary to quantitate potentially more subtle changes in the occupancy of these other sites and to determine their relevance to nitrite treatment.

Discussion

This study provides novel insights into the dose-response relationship, potential mechanisms, and consequences of nitrite-induced delayed cardioprotection. The principal findings are that: a) Acute systemic elevations in nitrite availability lead to transient increases in cardiac tissue nitrite and nitros(yl)lation. b) Despite this transiency, there is robust persisting myocellular oxidant stress, as manifested by the ascorbate oxidation status (DHA/AA); changes in the oxidation status of this redox couple are specific, as they are not reflected in total protein carbonylation, nor by the changes seen in the glutathione oxidation

status (GSSG/GSH) that follow a complex nitrite-dose response. c) These changes are associated with complex and specific alterations of proteins in key pathways, some of which are already known to have a role in cardioprotection.[26,27,29] Such pathways include: myofilament-related and energy consuming proteins (*e.g.* FLNC, α-actin, sarcomeric MLC), energy producing proteins (*e.g.*, LDH, PDC-E2), serine/threonine kinase signaling proteins (*e.g.* PKA and PP2A) and proteins modifying mitochondrial function and the response to redox stress (*e.g.*, PDIA3, COQ9, and ALDH2). d) Despite the complexity of the changes we observed in redox status and in the proteome, the same nitrite-dose related pattern was recapitulated in nitrite's delayed cardioprotection against I/R injury.

Previous studies have highlighted nitrite's ability to confer cardioprotection,[7–12] however the efficacy of nitrite in delayed cardioprotection (at 24 h) still remains to be explored. In particular, the dose-response relationship of nitrite-mediated cardioprotection and the mechanisms conferring its benefits remain to be determined. The present study suggests that systemic exposure to nitrite, such as that which occurs physiologically (*e.g.*, with exercise[4,30]), results in rapid uptake and metabolism of nitrite by the heart. Despite the transient nature of increases in tissue nitrite and consequent nitros(yl)ation levels, these changes induce a protracted influence on tissue redox status. Acute nitrite exposure increases the ascorbate oxidation status (DHA/AA) over 48 h and alters the glutathione oxidation status (GSSG/GSH) in a complex nitrite dose-dependent manner. The importance of these changes is underlined by the observation that there is a compelling correspondence between the pattern of GSSG/GSH changes and contractile recovery following myocardial ischemia and reperfusion *ex vivo*.

Although the explanation for these redox changes is yet to be investigated, we speculate (Fig. 7) that these changes reflect the influence of nitrite on nitric oxide (NO) and reactive oxygen species (ROS) availability, cross-talk, and signaling. Although both NO and ROS are known to fulfill critical cell signaling functions, it appears that both the level and the balance of these species, and their interaction to form peroxynitrite (ONOO), are critical in determining whether cells exhibit a detrimental or beneficial delayed preconditioning response.[31] Moreover, a significant body of literature suggests that both species are necessary to trigger delayed protection.[31,32] The association between glutathione oxidation status and myocardial recovery from I/R injury raises the possibility that the dose-dependent modulation of redox status by transient nitrite exposure is pertinent to cardioprotection.

Concurrent with these persisting redox and functional changes, the heart undergoes significant proteomic changes in response to brief nitrite exposure. Alterations in the expression pattern of protein isoforms (*e.g.*, isoforms of PDIA3, COQ9, and ALDH2) have been identified in the context of nitrite exposure for the first time. Many of these proteins and the pathways to which they belong have recently been identified as critical mediators of cardioprotection arising from different preconditioning stimuli, underlining the robustness of conserved preconditioning pathways.[26,27,29,33,34] Moreover, LC-MS of peptides from pooled nitrite-treated versus control animals demonstrated specific nitrite-induced protein phosphorylation (*e.g.* ALDH2, FLNC, PKA, and PP2A). It is noteworthy that the phosphorylation of ALDH2 at Thr431 that we observed has been described as being regulated by protein kinase Cε (PKCε) activity and has been linked to cardioprotective

increases in ALDH2 enzymatic activity.[34] Future studies will be necessary to quantitate the nitrite-dose response of the phosphosites we have described and to probe deeper into the proteome to investigate the quantitative changes, stoichiometry and functional consequences of putative phosphorylation elicited by nitrite (*e.g.* in myofilament proteins, MLC1) and their relationship to cardioprotection. Additionally, other functional PTMs[26,27,29,35] (*e.g.* prolyl hydroxylation, oxidation, *N*-acetylglucosamine modification) should be investigated by methodologies tailored to their enrichment and characterization.

In accordance with other similar studies,[26,27,29] novel and important, hypothesis-generating information has been gained from relatively unbiased proteomic investigations. In contrast to most cardioprotection proteomic analyses performed to date using isolated myocytes explanted 60 min after treatment, our studies were performed on whole heart preparations and uniquely studied the metabolome/proteome long after treatment (at 24 h), yielding novel insights into potential mediators and pathways of late cardioprotection. Despite our extensive 2D-PAGE approach using cell compartment-specific proteomics, the protein changes identified are by no means comprehensive. For technical reasons (*e.g.* the high dynamic range of protein abundances, the limited compatibility of 2D-PAGE methodologies with large and hydrophobic proteins, *etc.*) such proteomic approaches only provide a limited window into the biological pathways involved.[26] Thus, many of the observations reported herein represent only the first stage of full structural and functional determination of nitrite-dependent protein alterations. Precise sites (and in some cases, types) of PTMs on many of the proteins (*e.g.*, PDIA3, COQ9, additional sites on ALDH2) remain uncharacterized. Future analyses should enable the identification of these PTMs and the determination as to whether they are stimulatory or inhibitory to protein function. For example, the changes in post-translational modification of myofilament proteins will need to be characterized comprehensively, and detailed functional assays will need to be performed to determine their contribution to cardioprotection.[36,37] Specifically, issues of the stoichiometry of myofilament PTMs (namely, the extent of modification of the total myofilament protein pool and how this may impact function *in vivo*) will have to be addressed. Such PTMs, if present with sufficient stoichiometry, may make an important contribution to sarcomeric function and hence may contribute to alterations in energetic state during I/R. Finally, although beyond the scope of this largely proteomic study, it will be necessary to test the hypothesis that the elaboration of NO and ROS are pertinent to delayed nitrite-induced cardioprotection. This may be accomplished through the systematic assessment of the response to I/R following the concurrent administration of nitrite and antioxidants (*e.g.*, superoxide dismutase, catalase, and mercaptopropionyl glycine).[32,38,39] Bearing in mind nitrite's direct and indirect capacity for protein modification, comprehensive strategies will be needed to dissect out the role(s) of such changes in nitrite-mediated cardioprotection.

Conclusions

The present study confirms that nitrite is an effective cardioprotective agent that can facilitate persistent protection against myocardial ischemia and reperfusion. We propose for the first time that: a) The protective influence of nitrite conforms to a complex dose-response relationship (only low and high doses are effective). b) These doses induce a complex oxidant stress pattern with oxidized ascorbate and reduced glutathione corresponding to a

functionally protected heart. c) The changes in redox status not only correlate with functional protection, but also correspond to a complex pattern of putatively protective protein alterations, including PTMs (phosphorylaton and nitration), of proteins involved in serine/threonine kinase signaling, protection from oxidative stress, potential bioconversion of nitrite to NO, and proteins involved in the cellular metabolic machinery that ensures an optimal energetic balance. Although further studies will be needed to fully delineate the mechanisms of nitrite-induced cardioprotection, this study informs ongoing basic and translational studies by highlighting the importance of the dose-effect relationship for nitrite and the broad array of downstream targets possibly involved in its cardioprotective efficacy (Fig. 7). Finally, our results may be of relevance to discussions about the role of lifestyle-related factors for cardiovascular health, in the context of the transient increases in circulating nitrite levels following physical exercise[30] and ingestion of nitrite/nitrate-rich foods.[3]

Supplementary Material

Refer to Web version on PubMed Central for supplementary material.

Acknowledgements

This project was supported by NIH grants P41 RR10888 (to CEC), S10 RR15942 (to CEC), S10 RR20946 (to J Zaia), and R01 HL69029 (to MF), and NHLBI contract N01 HV28178 (to CEC).

Reference List

1. Mazzone M, Carmeliet P. Drug discovery: a lifeline for suffocating tissues. Nature. 2008;453:1194–1195. [PubMed: 18580938]
2. Zweier JL, Wang P, Samouilov A, Kuppusamy P. Enzyme-independent formation of nitric oxide in biological tissues. Nat Med. 1995;1:804–809. [PubMed: 7585184]
3. Lundberg JO, Weitzberg E, Gladwin MT. The nitrate-nitrite-nitric oxide pathway in physiology and therapeutics. Nat Rev Drug Discov. 2008;7:156–167. [PubMed: 18167491]
4. Cosby K, Partovi KS, Crawford JH, Patel RP, Reiter CD, Martyr S, Yang BK, Waclawiw MA, Zalos G, Xu X, Huang KT, Shields H, Kim-Shapiro DB, Schechter AN, Cannon RO III, Gladwin MT. Nitrite reduction to nitric oxide by deoxyhemoglobin vasodilates the human circulation. Nat Med. 2003;9:1498–1505. [PubMed: 14595407]
5. Maher AR, Milsom AB, Gunaruwan P, Abozguia K, Ahmed I, Weaver RA, Thomas P, Ashrafian H, Born GV, James PE, Frenneaux MP. Hypoxic modulation of exogenous nitrite-induced vasodilation in humans. Circulation. 2008;117:670–677. [PubMed: 18212289]
6. Kumar D, Branch BG, Pattillo CB, Hood J, Thoma S, Simpson S, Illum S, Arora N, Chidlow JH Jr., Langston W, Teng X, Lefer DJ, Patel RP, Kevil CG. Chronic sodium nitrite therapy augments ischemia-induced angiogenesis and arteriogenesis. Proc Natl Acad Sci U S A. 2008;105:7540–7545. [PubMed: 18508974]
7. Shiva S, Sack MN, Greer JJ, Duranski M, Ringwood LA, Burwell L, Wang X, MacArthur PH, Shoja A, Raghavachari N, Calvert JW, Brookes PS, Lefer DJ, Gladwin MT. Nitrite augments tolerance to ischemia/reperfusion injury via the modulation of mitochondrial electron transfer. J Exp Med. 2007;204:2089–2102. [PubMed: 17682069]
8. Gonzalez FM, Shiva S, Vincent PS, Ringwood LA, Hsu LY, Hon YY, Aletras AH, Cannon RO III, Gladwin MT, Arai AE. Nitrite anion provides potent cytoprotective and antiapoptotic effects as adjunctive therapy to reperfusion for acute myocardial infarction. Circulation. 2008;117:2986–2994. [PubMed: 18519850]

9. Bryan NS, Calvert JW, Gundewar S, Lefer DJ. Dietary nitrite restores NO homeostasis and is cardioprotective in endothelial nitric oxide synthase-deficient mice. Free Radic Biol Med. 2008.
10. Bryan NS, Calvert JW, Elrod JW, Gundewar S, Ji SY, Lefer DJ. Dietary nitrite supplementation protects against myocardial ischemia-reperfusion injury. Proc Natl Acad Sci U S A. 2007;104:19144–19149. [PubMed: 18025468]
11. Duranski MR, Greer JJ, Dejam A, Jaganmohan S, Hogg N, Langston W, Patel RP, Yet SF, Wang X, Kevil CG, Gladwin MT, Lefer DJ. Cytoprotective effects of nitrite during in vivo ischemia-reperfusion of the heart and liver. J Clin Invest. 2005;115:1232–1240. [PubMed: 15841216]
12. Shiva S, Huang Z, Grubina R, Sun J, Ringwood LA, MacArthur PH, Xu X, Murphy E, Darley-Usmar VM, Gladwin MT. Deoxymyoglobin is a nitrite reductase that generates nitric oxide and regulates mitochondrial respiration. Circ Res. 2007;100:654–661. [PubMed: 17293481]
13. Gladwin MT, Kim-Shapiro DB. The functional nitrite reductase activity of the heme-globins. Blood. 2008.
14. Li H, Cui H, Kundu TK, Alzawahra W, Zweier JL. Nitric oxide production from nitrite occurs primarily in tissues not in the blood: critical role of xanthine oxidase and aldehyde oxidase. J Biol Chem. 2008;283:17855–17863. [PubMed: 18424432]
15. Benjamin N, O'Driscoll F, Dougall H, Duncan C, Smith L, Golden M, McKenzie H. Stomach NO synthesis. Nature. 1994;368:502.
16. Webb A, Bond R, McLean P, Uppal R, Benjamin N, Ahluwalia A. Reduction of nitrite to nitric oxide during ischemia protects against myocardial ischemia-reperfusion damage. Proc Natl Acad Sci U S A. 2004;101:13683–13688. [PubMed: 15347817]
17. Gladwin MT, Schechter AN, Kim-Shapiro DB, Patel RP, Hogg N, Shiva S, Cannon RO III, Kelm M, Wink DA, Espey MG, Oldfield EH, Pluta RM, Freeman BA, Lancaster JR Jr., Feelisch M, Lundberg JO. The emerging biology of the nitrite anion. Nat Chem Biol. 2005;1:308–314. [PubMed: 16408064]
18. Ferrara N, Bohm M, Zolk O, O'Gara P, Harding SE. The role of Gi-proteins and beta-adrenoceptors in the age-related decline of contraction in guinea-pig ventricular myocytes. J Mol Cell Cardiol. 1997;29:439–448. [PubMed: 9140804]
19. Bryan NS, Rassaf T, Maloney RE, Rodriguez CM, Saijo F, Rodriguez JR, Feelisch M. Cellular targets and mechanisms of nitros(yl)ation: an insight into their nature and kinetics in vivo. Proc Natl Acad Sci U S A. 2004;101:4308–4313. [PubMed: 15014175]
20. Feelisch M, Rassaf T, Mnaimneh S, Singh N, Bryan NS, Jourd'Heuil D, Kelm M. Concomitant S-, N-, and heme-nitros(yl)ation in biological tissues and fluids: implications for the fate of NO in vivo. FASEB J. 2002;16:1775–1785. [PubMed: 12409320]
21. Perlman DH, Berg EA, O'connor PB, Costello CE, Hu J. Reverse transcription-associated dephosphorylation of hepadnavirus nucleocapsids. Proc Natl Acad Sci U S A. 2005;102:9020–9025. [PubMed: 15951426]
22. Zhang X, Ye J, Jensen ON, Roepstorff P. Highly efficient phosphopeptide enrichment by calcium phosphate precipitation combined with subsequent IMAC enrichment. Mol Cell Proteomics. 2007;6:2032–2042. [PubMed: 17675664]
23. Thingholm TE, Jorgensen TJ, Jensen ON, Larsen MR. Highly selective enrichment of phosphorylated peptides using titanium dioxide. Nat Protoc. 2006;1:1929–1935. [PubMed: 17487178]
24. Licht WR, Tannenbaum SR, Deen WM. Use of ascorbic acid to inhibit nitrosation: kinetic and mass transfer considerations for an in vitro system. Carcinogenesis. 1988;9:365–372. [PubMed: 3345578]
25. Bryan NS, Fernandez BO, Bauer SM, Garcia-Saura MF, Milsom AB, Rassaf T, Maloney RE, Bharti A, Rodriguez J, Feelisch M. Nitrite is a signaling molecule and regulator of gene expression in mammalian tissues. Nat Chem Biol. 2005;1:290–297. [PubMed: 16408059]
26. Arrell DK, Elliott ST, Kane LA, Guo Y, Ko YH, Pedersen PL, Robinson J, Murata M, Murphy AM, Marban E, Van Eyk JE. Proteomic analysis of pharmacological preconditioning: novel protein targets converge to mitochondrial metabolism pathways. Circ Res. 2006;99:706–714. [PubMed: 16946135]

27. Arrell DK, Neverova I, Fraser H, Marban E, Van Eyk JE. Proteomic analysis of pharmacologically preconditioned cardiomyocytes reveals novel phosphorylation of myosin light chain 1. Circ Res. 2001;89:480–487. [PubMed: 11557734]

28. Gharib M, Marcantonio M, Lehmann SG, Courcelles M, Meloche S, Verreault A, Thibault P. Artifactual sulfation of silver-stained proteins: Implications for the assignment of phosphorylation and sulfation sites. Mol Cell Proteomics. 2008.

29. Mayr M, Liem D, Zhang J, Li X, Avliyakulov NK, Yang JI, Young G, Vondriska TM, Ladroue C, Madhu B, Griffiths JR, Gomes A, Xu Q, Ping P. Proteomic and metabolomic analysis of cardioprotection: Interplay between protein kinase C epsilon and delta in regulating glucose metabolism of murine hearts. J Mol Cell Cardiol. 2008.

30. Rassaf T, Lauer T, Heiss C, Balzer J, Mangold S, Leyendecker T, Rottler J, Drexhage C, Meyer C, Kelm M. Nitric oxide synthase-derived plasma nitrite predicts exercise capacity. Br J Sports Med. 2007;41:669–673. [PubMed: 17496072]

31. Ferdinandy P, Schulz R. Nitric oxide, superoxide, and peroxynitrite in myocardial ischaemia-reperfusion injury and preconditioning. Br J Pharmacol. 2003;138:532–543. [PubMed: 12598407]

32. Bolli R Preconditioning: a paradigm shift in the biology of myocardial ischemia. Am J Physiol Heart Circ Physiol. 2007;292:H19–H27. [PubMed: 16963615]

33. Churchill EN, Disatnik MH, Mochly-Rosen D. Time-dependent and ethanol-induced cardiac protection from ischemia mediated by mitochondrial translocation of var epsilon PKC and activation of aldehyde dehydrogenase 2. J Mol Cell Cardiol. 2008.

34. Chen CH, Budas GR, Churchill EN, Disatnik MH, Hurley TD, Mochly-Rosen D. Activation of aldehyde dehydrogenase-2 reduces ischemic damage to the heart. Science. 2008;321:1493–1495. [PubMed: 18787169]

35. Ramirez-Correa GA, Jin W, Wang Z, Zhong X, Gao WD, Dias WB, Vecoli C, Hart GW, Murphy AM. O-linked GlcNAc modification of cardiac myofilament proteins: a novel regulator of myocardial contractile function. Circ Res. 2008;103:1354–1358. [PubMed: 18988896]

36. Marston SB, Redwood CS. Modulation of thin filament activation by breakdown or isoform switching of thin filament proteins: physiological and pathological implications. Circ Res. 2003;93:1170–1178. [PubMed: 14670832]

37. Kentish JC, McCloskey DT, Layland J, Palmer S, Leiden JM, Martin AF, Solaro RJ. Phosphorylation of troponin I by protein kinase A accelerates relaxation and crossbridge cycle kinetics in mouse ventricular muscle. Circ Res. 2001;88:1059–1065. [PubMed: 11375276]

38. Tang XL, Takano H, Rizvi A, Turrens JF, Qiu Y, Wu WJ, Zhang Q, Bolli R. Oxidant species trigger late preconditioning against myocardial stunning in conscious rabbits. Am J Physiol Heart Circ Physiol. 2002;282:H281–H291. [PubMed: 11748073]

39. Takano H, Tang XL, Qiu Y, Guo Y, French BA, Bolli R. Nitric oxide donors induce late preconditioning against myocardial stunning and infarction in conscious rabbits via an antioxidant-sensitive mechanism. Circ Res. 1998;83:73–84. [PubMed: 9670920]

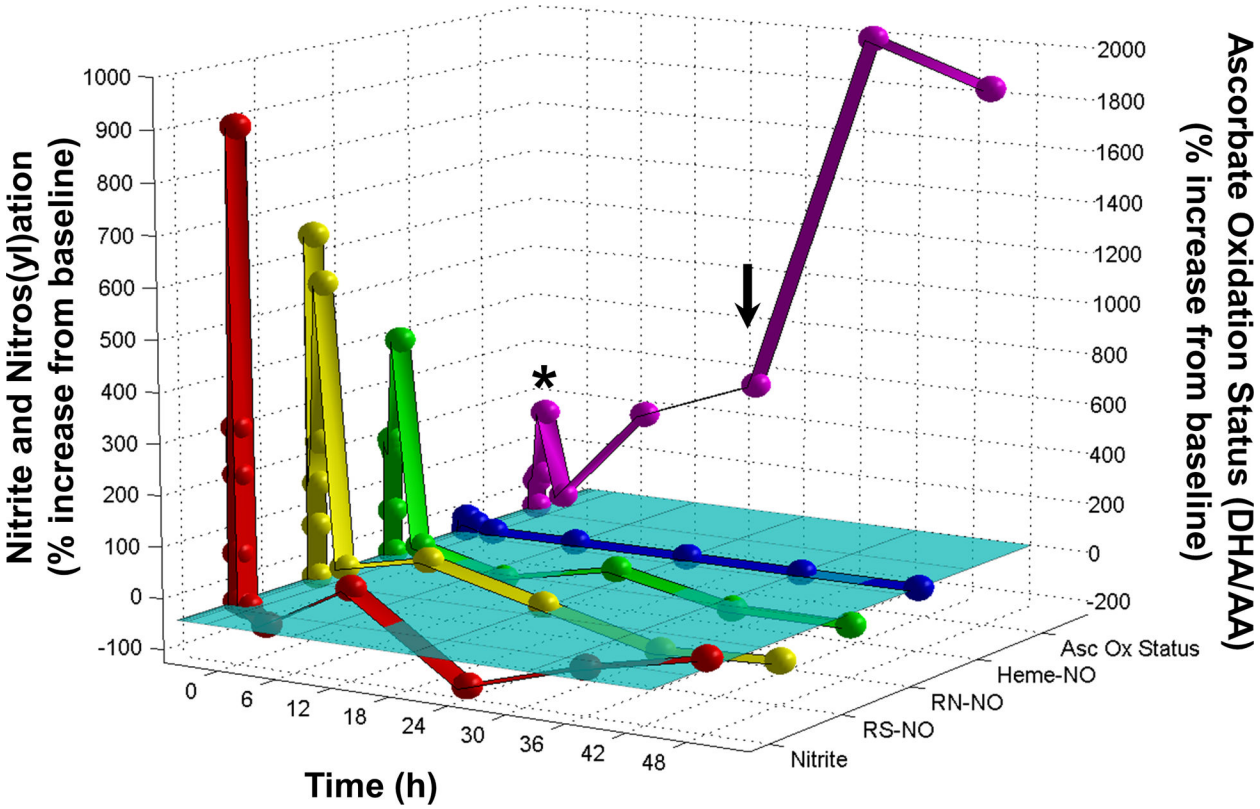

Figure 1. Major, long-term perturbation of cardiac redox tone following brief elevations in nitrite.

Detailed examination of the levels of cardiac nitrite, *S*- and *N*- nitroso and heme-nitrosyl species, and ascorbate oxidation status through time after a brief systemic nitrite elevation. Hearts from animals administered a bolus dose of nitrite (1 mg/kg) by intraperitoneal injection were analyzed after 0, 2, 5, 10, and 30 min, and 1, 3, 12, 24, 36, and 48 h. Cardiac nitrite levels were determined by ion chromatography; *S*-nitrosothiol (RS-NO), *N*-nitrosamine (RN-NO) and heme nitrosylation (heme-NO) levels were determined by gas-phase chemiluminescence; the ascorbate oxidation status, *i.e.* the ratio of dehydroascorbate (DHA) over ascorbic acid (AA), was determined by spectrophotometry. Values are normalized as percent change from baseline, which is indicated by the cyan plane. Left axis, nitrite and nitros(yl)ation scale; right axis, ascorbate oxidation status scale. The asterisk indicates the brief elevation in ascorbate oxidation status that accompanies the spike in cardiac nitrite levels, while the arrow indicates the 24 h value during the subsequent protracted elevation of the ascorbate oxidation status (mean values of 3 animals/time point; error bars omitted for sake of clarity). Errors were all < ± 15 %.

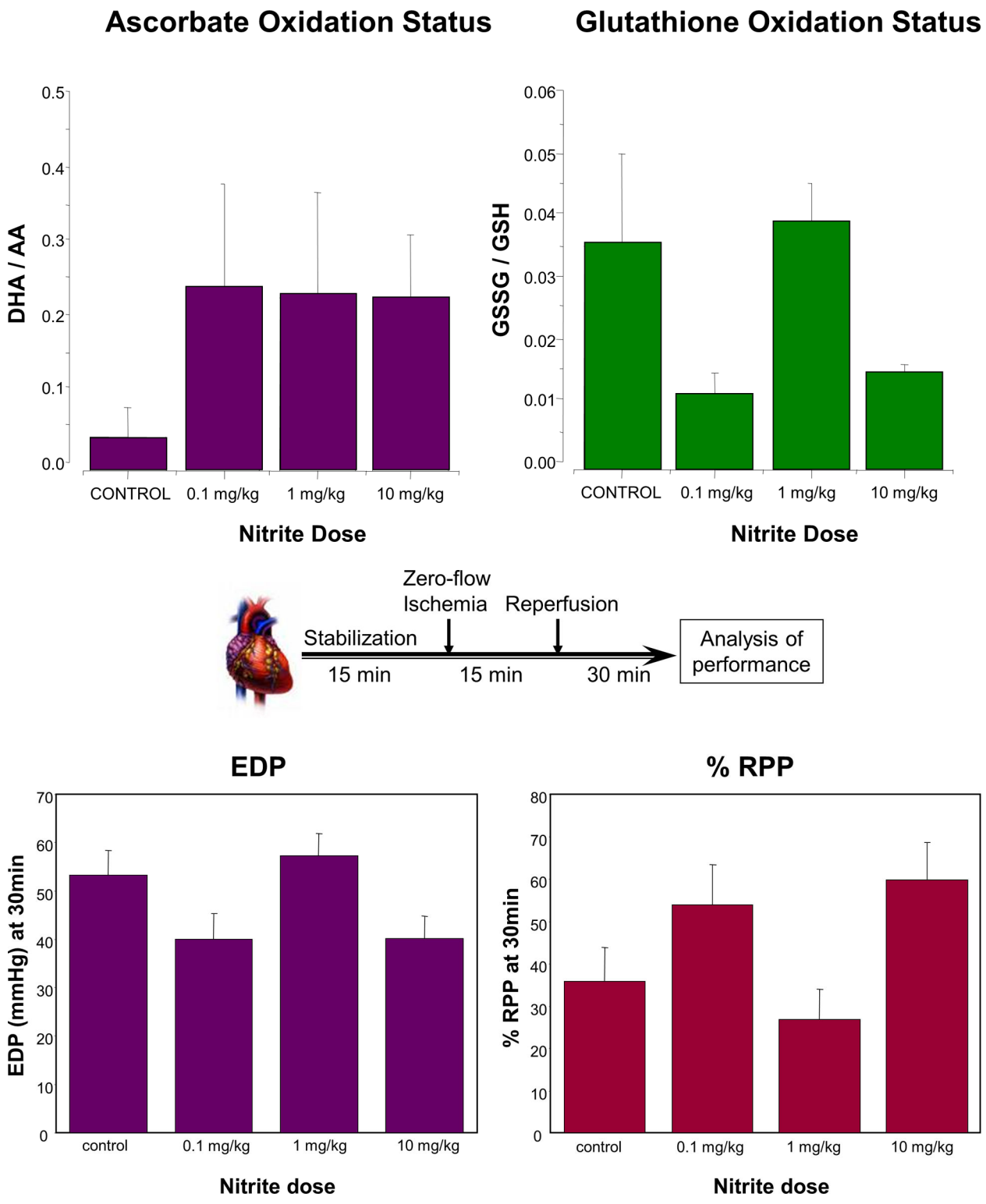

Figure 2. Complex dose-response of nitrite-induced long-term perturbations in cardiac redox tone and in cardiac preconditioning.

(A) Ascorbate oxidation uniformly increases in response to nitrite 24 h post administration, whereas the dose-response relationship of glutathione oxidation status is complex. Hearts

from animals administered a bolus dose of nitrite (0.1, 1.0, 10 mg/kg nitrite, or saline (control)) by intraperitoneal injection were analyzed after 24 h: the ascorbate oxidation status (DHA/AA) (left panel) and glutathione oxidation status (GSSG/GSH) (right panel) were determined by spectrophotometric methods (means ± SEM; n = 3). (B) Dose-dependent cardioprotective or detrimental preconditioning by nitrite. Hearts, isolated from animals 24 h after administration of a bolus dose of nitrite (0.1, 1.0, 10 mg/kg nitrite, or saline (control)), were perfused in the Langendorff mode, subjected to *ex vivo* ischemia/reperfusion, and monitored for recovery of contractile function: after 15 min of stabilization, hearts were subjected to 15 min of global ischemia, followed by 30 min of reperfusion, at which time end diastolic pressure (EDP), rate/pressure product (RPP) and other hemodynamic parameters were measured (mean values ± SEM; n = 4–5).

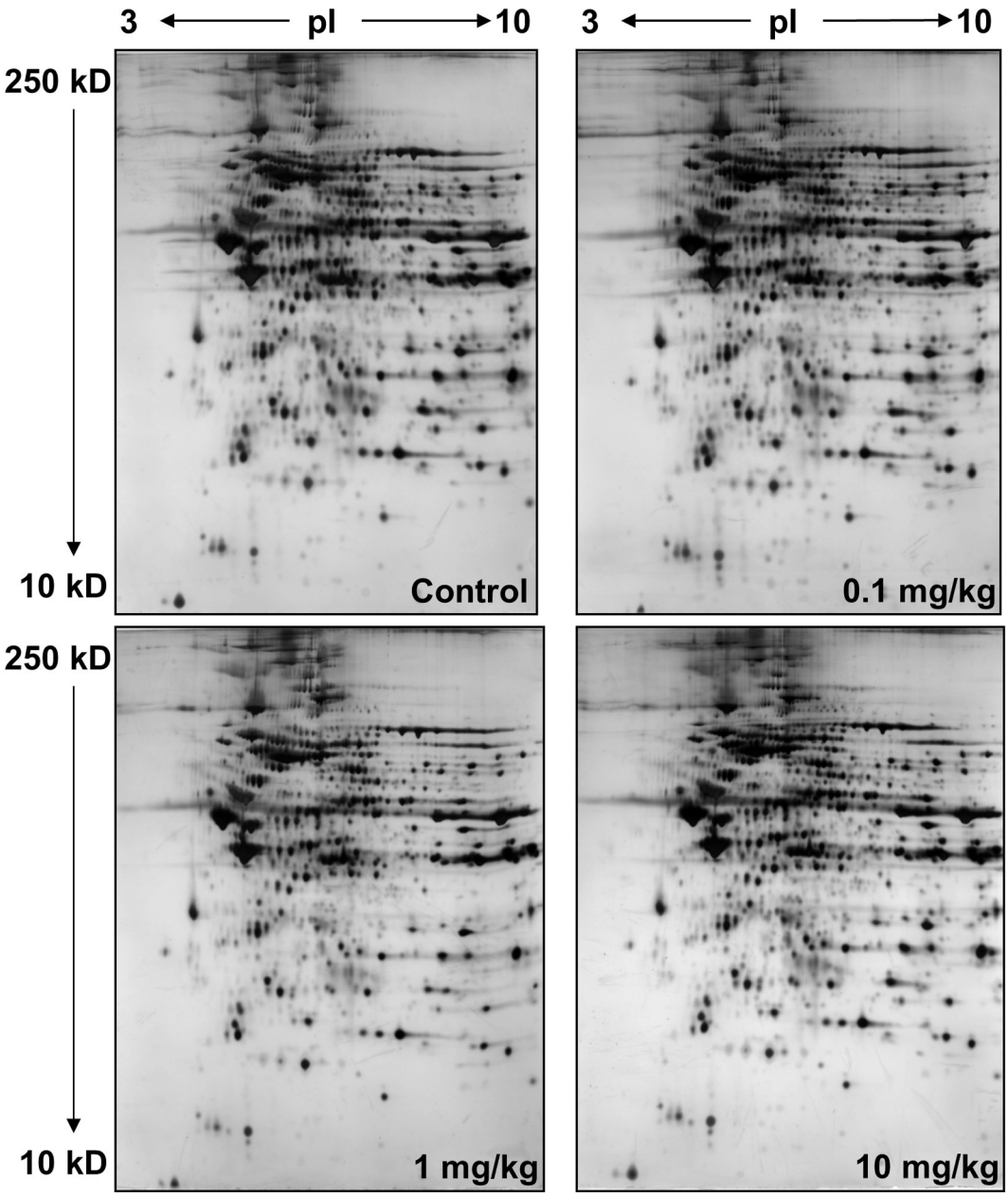

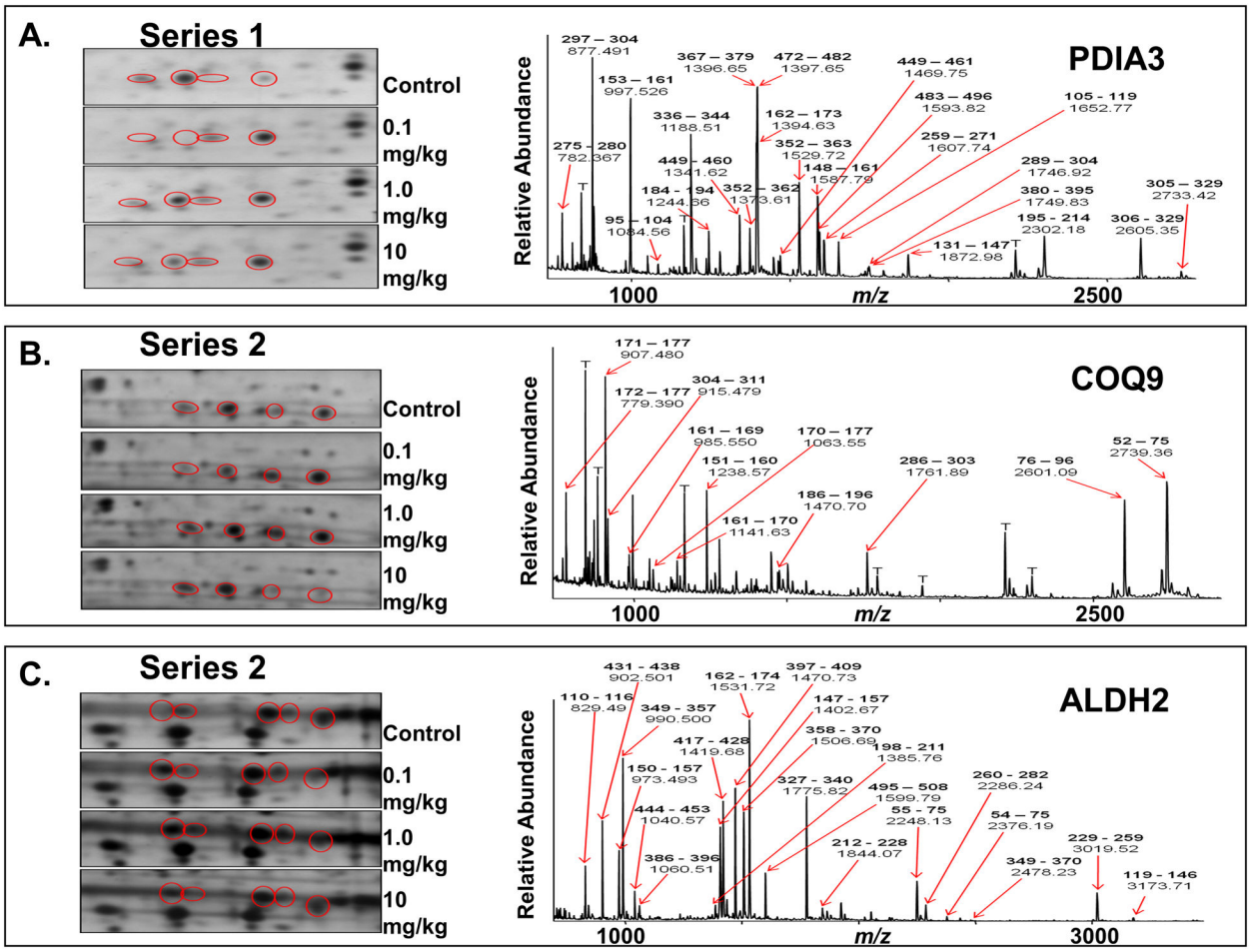

Figure 3. Nitrite-induced alterations to cardiac mitochondrial-associated proteins, PDIA3, COQ9, and ALDH2, revealed by differential 2D-PAGE and MS analyses.

Hearts from animals administered a bolus dose of nitrite (0.1, 1.0, 10 mg/kg nitrite, or saline (control)) were isolated 24 h post administration, homogenized and subjected to differential centrifugation to isolate mitochondria and post-mitochondrial cytoplasmic supernatant. Protein was subjected to 2D-PAGE and visualized by silver staining. All samples were pooled from 3 animals per dose; gels are representative of a minimum of three replicates. (A) Purified cardiac mitochondria (50 μg), subjected to 2D-PAGE over the pI range 3–10 and molecular weight (mw) range of approximately 250–10 kD, as indicated (shown to display uniformity of preparation and staining). (B) Enlargments across treatment groups of 3 regions of 2D gels run with the same mitochondrial material as in (A) over the pI range 4–7 and mw range of approximately 250–10 kD (enlargements, left panels; full gels, Fig. S-2, Online Data Supplement). Spots circled in red are constituents that appeared to be grossly differentially expressed at different levels of nitrite exposure. (i) Series 1, train of 4 spots, labeled a-d, at ca. pI 6 and mw 60 kD. (ii) Series 2, train of 4 spots, labeled a-d, at ca. pI 5 and mw 30 kD. (iii) Series 3, train of 5 spots, labeled a-e, at ca. pI 6.3 and mw 57 kD. A summary of the changes observed in these 3 series of spots can be found in Table 2 (Online Data Supplement). The same spots from equivalent 2D–PAGE gels (using ~10-fold more protein) stained with Coomassie blue were excised and subjected to in-gel digestion. Eluted

peptides were analyzed by MALDI-TOF MS, and resultant spectra (right panels; spectra shown for one spot in each series over the approximate range *m/z* 700–3000) were analyzed to generate peptide ion peak lists that were submitted to the on-line database search engine, Mascot™, for peptide mass fingerprint analyses against the rat proteomic database. Spots series 1, 2, and 3, were determined to consist of isoforms of protein disulfide isomerase A3 (Mascot score, 221; expect value 1.6×10^{-18}), ubiquinone biosynthesis protein CoQ9 (Mascot score, 79; expect value 8.6×10^{-5}), and aldehyde dehydrogenase 2 (Mascot score, 205; expect value 6.2×10^{-17}), respectively. Prominent peptide ions are labeled in the spectra with their observed *m/z* values and corresponding amino acid intervals (bold) within the sequence of the assigned proteins. T, trypsin autolysis peptide.

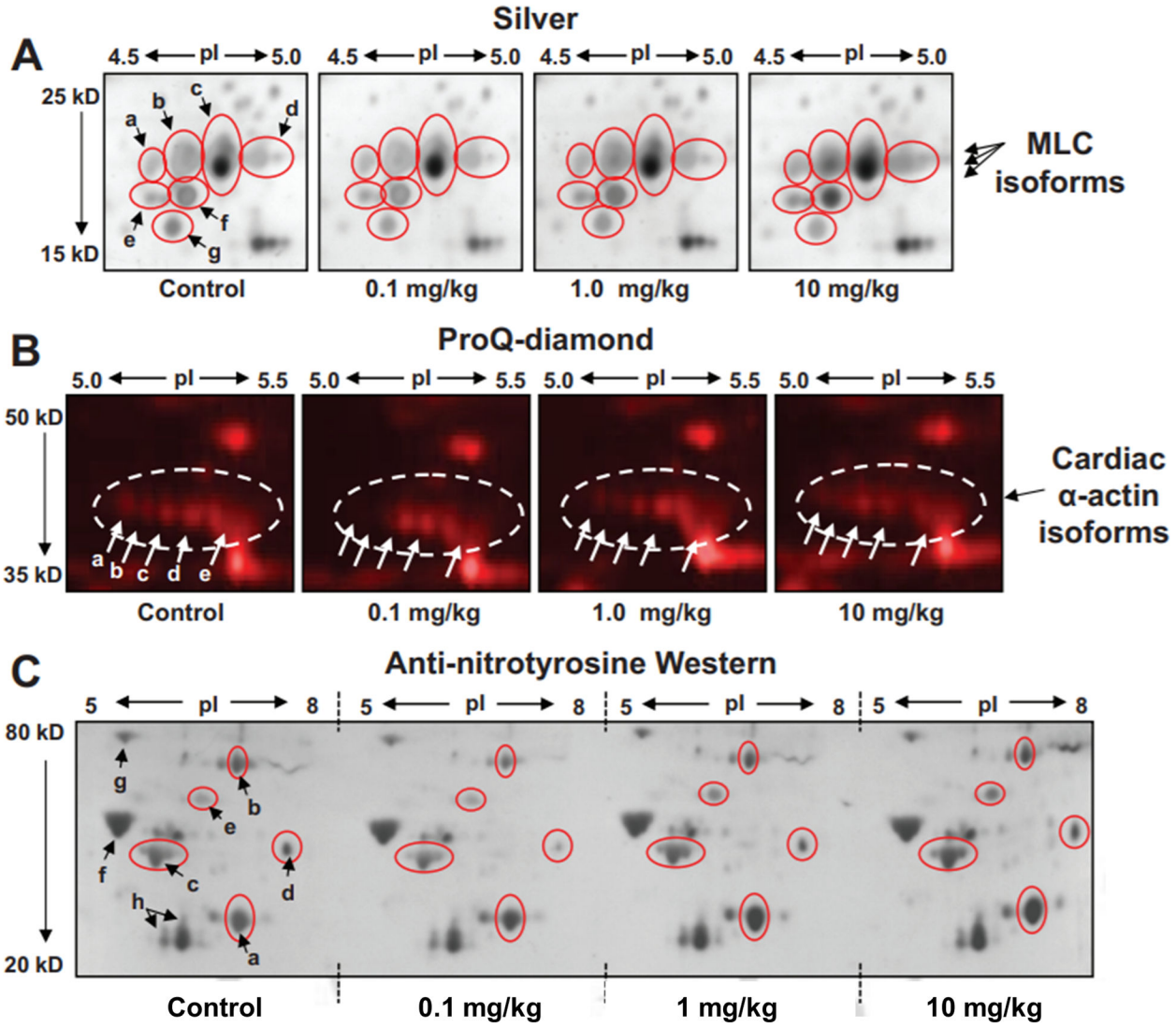

Figure 4. Alterations to other cardiac proteins, including myofilament, energetic, and signaling proteins induced by brief nitrite exposure.

Post-mitochondrial cytoplasmic supernatant purified by differential centrifugation from the cardiac tissue of animals administered a bolus dose of 0.1, 1.0, 10 mg/kg nitrite, or saline (control), as described, was analyzed by 2D-PAGE over the pI range 4–7 and molecular weight range of 250–10 kD. Shown here (A) are enlargements of the myosin light chain 1 (MLC1) region displaying differential changes in isoform expression (spots a-g, circled in red) depending on nitrite dose. (B) Equivalent gels were run and stained with the phosphoprotein-sensitive fluorescent dye, ProQ-Diamond™. Shown are enlargements of the actin region (actin circled) displaying differential changes in actin migrational isoforms (spots labeled a-e) according to nitrite dose. (C) Changes in protein nitration due to acute nitrite exposure. Equivalent amounts of cardiac tissue homogenate from animals administered a bolus dose of 0.1, 1.0, 10 mg/kg nitrite, or saline (control), were analyzed by IEF over the pI range 3–10. IEF strips were trimmed to pI ranges of 5–8 and then placed alongside one another atop a single second dimension gel and subjected to SDS-PAGE

followed by Western blotting of a single membrane using anti-nitrotyrosine anti-sera. Shown is the 2D-Western blot over the molecular weight range of 80–20 kD. Nitrotyrosine–related immunoreactive protein spots a-h (a-e, changing with nitrite dose, circled in red). a) lactate dehydrogenase B (LDH), b) dehydrolipamide *S*-acetyl transferase (PDC-E2), c) actin, d) & e) unidentified cardiac proteins, f) F1 ATPase beta subunit, g) GRP78, h) MLC isoforms.

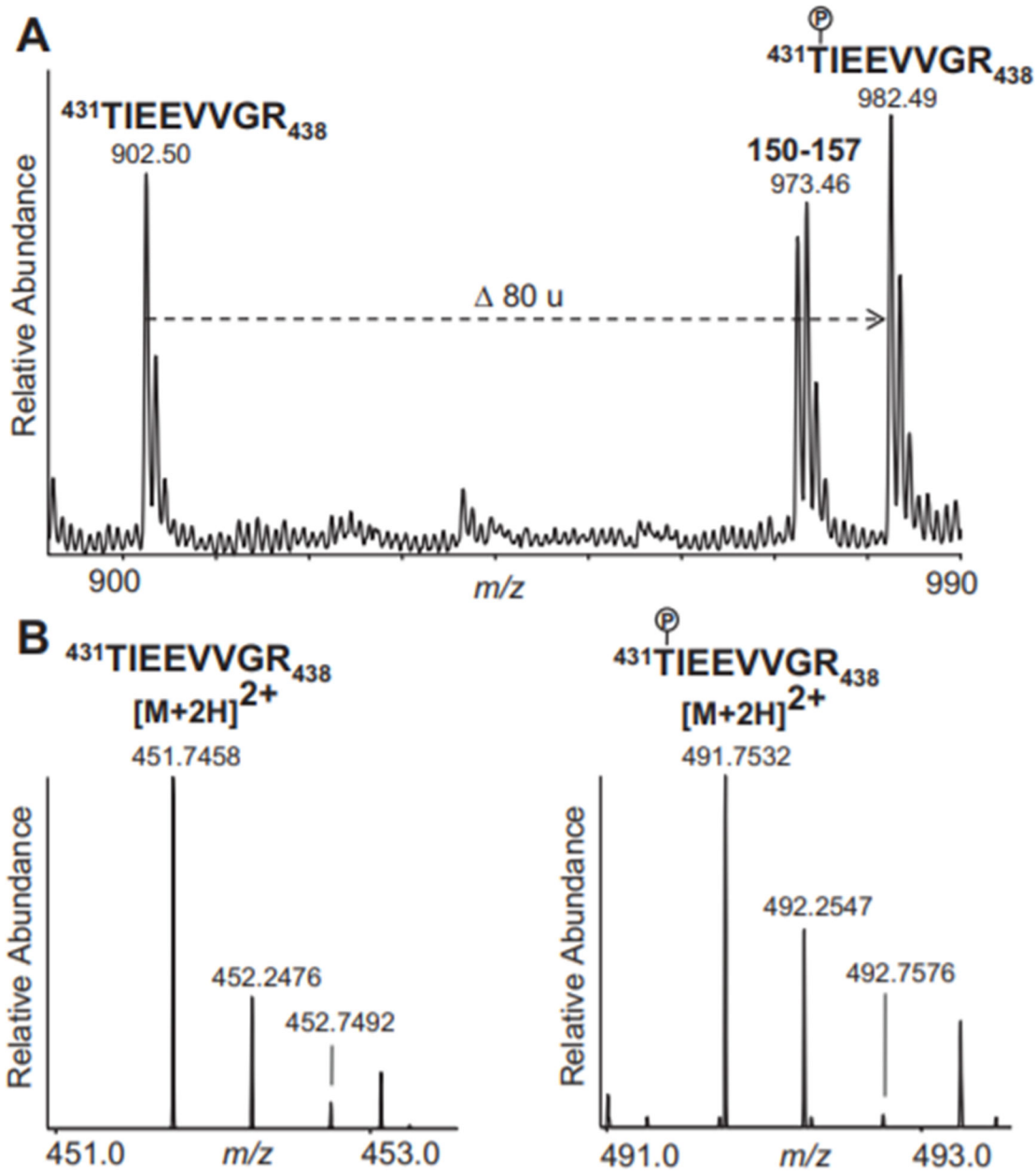

Figure 5. Phosphorylated and non-phosphorylated forms of ALDH2 peptide ^{431}TIEEVVGR$_{438}$ detected by MS analyses.

Ions are labeled with their detected *m/z* values. The phosphorylated Thr431 residue is indicated on the sequences with a P inside a circle. (A) MALDI-TOF mass spectrum of peptides from a spot assigned by PMF to ALDH2 in the 2D-PAGE analysis of mitochondria from nitrite-treated animals (as in Fig 3Biii, spot b), shown over the range *m/z* 900–990. Labeled are the unmodified ALDH2 peptide, 431–438, the phosphorylated species of the same peptide (the shift of 80 u corresponding to the addition of a phosphate group), and another ALDH2 peptide, 150–157. (B) ESI mass spectra recorded during LC-MS analysis of peptides that were isolated, through in-solution digestion and phosphopeptide enrichment, directly from pooled heart homogenates of nitrite-treated animals. Shown are regions of the

mass spectra containing the $[M+2H]^{2+}$ molecular ions assigned to the unmodified (left panel; displaying the range *m/z* 451.0–453.0) and the phosphorylated (right panel; displaying the range *m/z* 491.0–493.0) species of the ALDH2 peptide, 431–438.

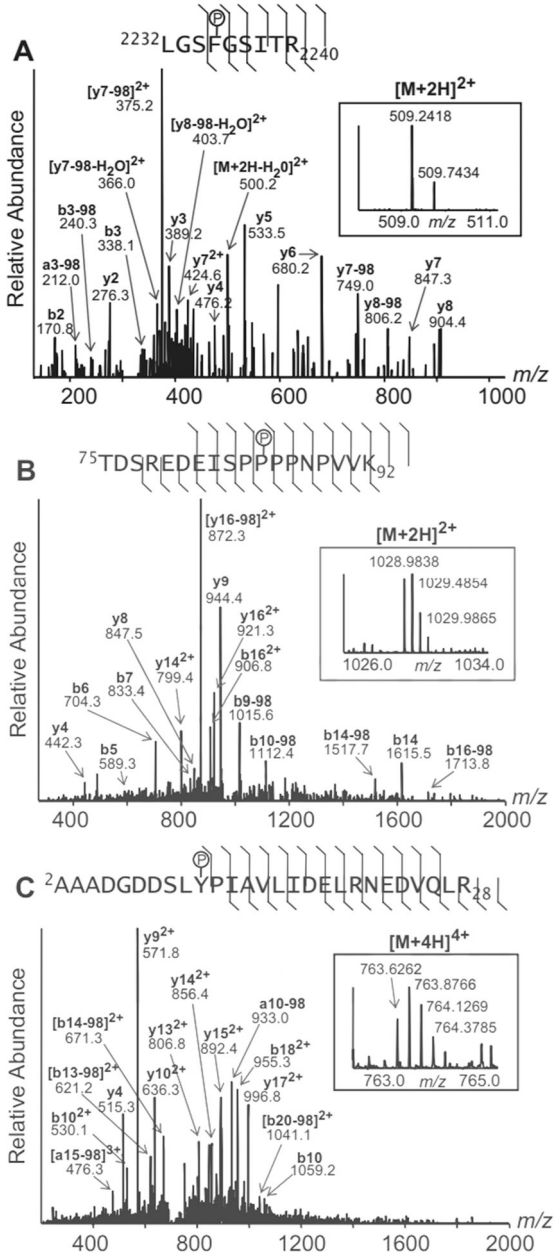

Figure 6. Phosphospecies of filamin-C, PKA, and PP2A subunits detected differentially in heart homogentes of nitrite-treated animals.

Tandem mass spectra from three phosphopeptides which were present differentially in homogenates of nitrite-treated animals. (A) Filamin-C (FLNC) phosphopeptide corresponding to amino acids 2232–2240, containing phosphorylated Ser2234 ($[M+2H]^{2+}$ *m/z* 509.2418). (B) PKA Regulatory Subunit 1-alpha (KAP0) phosphopeptide, corresponding to amino acids 75–92, containing phosphorylated Ser83 ($[M+2H]^{2+}$ *m/z* 1028.9838). (C) PP2A Regulatory Subunit A-alpha (2AAA) phosphopeptide, corresponding to amino acids 2–28, containing phosphorylated Ser9 ($[M+4H]^{4+}$ *m/z* 763.6262). Precursor ion spectra are shown inset into the product ion spectra (both over the indicated *m/z* ranges). The precursor ions and prominent fragment ions are labeled in the spectra with their

observed *m/z* values; where applicable, their corresponding b/y-ion designations, charge states, and neutral losses of phosphoric acid (−98) are labeled (bold). A summary of the fragment ion data, including the less abundant fragment ions detected, is indicated on the phosphopeptide sequence above each spectrum. In each case, the site of phosphorylation (indicated with a P inside a circle) is identified unambiguously by numerous prominent diagnostic b- and/or y- ions.

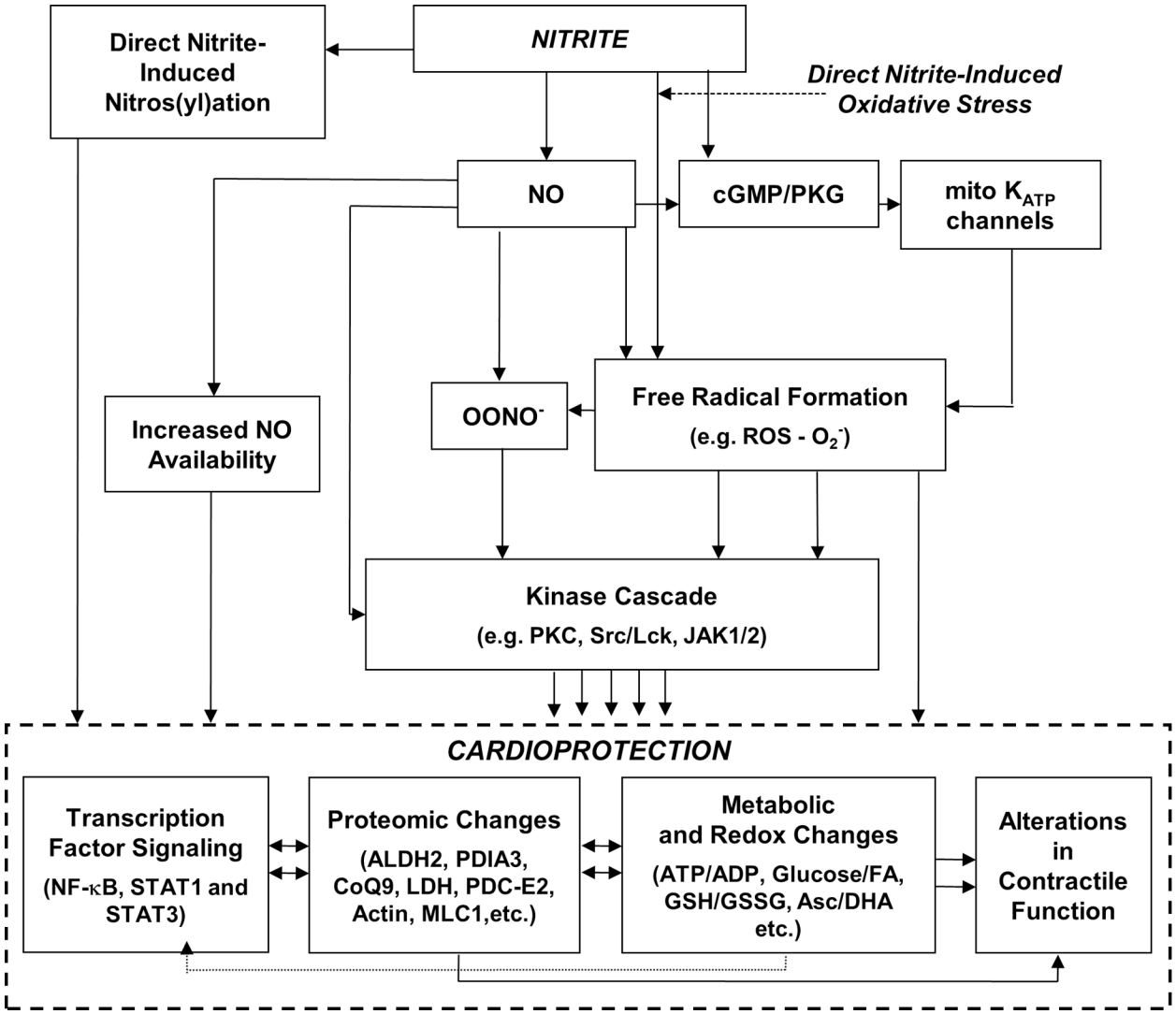

Figure 7. Schematic representation of the mechanisms underlying nitrite-induced late preconditioning.

Nitrite, both directly and through the release of NO, induces the release of free radicals, including reactive oxygen species (ROS). One mechanism leading to the increase in ROS includes NO-induced activation of cyclic GMP (cGMP) which in turn activates a redox-sensitive protein kinase G (PKG); this opens mitochondrial K_{ATP} channels, enhancing local ROS production. NO, ROS and peroxynitrite ($OONO^-$), when produced in an optimal balance resulting from effective nitrite concentrations and incipient conditions (*e.g.* cellular redox status), lead to activation of cellular kinases (*e.g.* PKA, PKC δ and ε). Nitrite-derived NO can also act via transient modification of components of the electron transport chain and *S*-nitrosation of proteins involved in regulation of mitochondrial energetics. Ultimately, these lead to cardioprotection mediated through the interplay of transcription factor signaling, proteomic, metabolic, and redox changes, and alterations in contractile function.